Large transboundary health impact of Arctic wildfire smoke

Check for updates

Ben Silver [1] ✉, Steve R. Arnold[1], Carly L. Reddington[1], Louisa K. Emmons [2] & Luke Conibear[1,3]

Rapid warming at high latitudes, particularly in Siberia, has led to large wildfires in recent years that cause widespread smoke plumes. These fires lead to substantial deterioration in summer air quality in the region, with a factor 4 increase in summer fine particulate matter ($PM_{2.5}$) concentrations in parts of Siberia during 1998–2020. Exposure to $PM_{2.5}$ is associated with increased risk of mortality due to cardiovascular and respiratory disease, and the atmospheric lifetime of $PM_{2.5}$ means that it can be efficiently transported between regions and nations. We used the Community Earth System Model to quantify the fraction of $PM_{2.5}$ attributed to high latitude wildfires that occur in the Arctic Council member states and estimated the attributable health impact locally and in neighbouring countries. During 2001–2020 we attribute ~21,000 excess deaths to Arctic Council wildfires on average each year, of which ~8000 occur in countries outside the Arctic Council. Our analysis shows that the health impact of Arctic wildfires decreased during 2001–2020, despite the increase of wildfire-sourced $PM_{2.5}$, which we suggest is due to a northwards shift in the average latitude of Siberian wildfires, reducing their impact on more densely populated regions.

The Arctic has warmed three times faster than the rest of the world during 1971–2019[1], with parts of Siberia warming even faster, making it one of the most rapidly warming areas in the world[2]. Warming in this region poses a potential climate risk due to the large stores of carbon contained in its ecosystems, peatlands, and permafrost soils[3]. During 2019 and 2020 unusually large wildfires in the Siberian Arctic burned almost half of the total area that had burned in the previous four decades[4,5], releasing an amount of carbon (in CO_2 equivalent terms) comparable with the emissions of France in 2019[6]. Arctic peatlands have historically acted as a carbon sink, but increased fire frequency and permafrost melting could convert them into a source during the coming century[7,8].

Globally, the area burned by fires has declined by around 25% over the period 1997–2013 according to satellite observations[9]. This is attributed to an increase in the proportion of land being used for agriculture, on which fires are more heavily supressed. Despite the burned area decline, the total carbon emitted from fires has remained stable, at around 2 Pg C year^{-1}, due to forest accounting for an increasing fraction of burned area, which has a greater carbon emission intensity than grassland[10]. Future climate change is likely to exacerbate this trend, especially in the Arctic, where increasing summer temperatures will render areas of boreal forest increasingly vulnerable to fire[11,12]. The frequency of peatland fires, which have the largest CO_2 emission intensity of all fire types[13], is predicted to increase in the Arctic boreal region[14]. Fire-

sourced carbon emissions could increase by a factor of 2–3 by 2100 in high latitude regions, including Siberia and Canada[14–16].

Wildfires in the Arctic are known to worsen air quality both in their immediate vicinity and in distant countries, due to the potential for smoke to be transported large distances in the atmosphere[17–19]. Wildfires produce primary air pollutants including particulate matter (i.e., smoke), carbon monoxide and polycyclic aromatic hydrocarbons, as well as contributing to secondary air pollution by emitting volatile organic compounds and nitrogen oxides, which can lead to tropospheric ozone formation, and the formation of secondary particulate matter[20–22]. Exposure to the fine fraction of particulate matter ($PM_{2.5}$), has been estimated to cause millions of deaths worldwide each year[23–25], with epidemiological evidence showing it elevates the risk of acute and chronic cardiovascular and respiratory disease[26,27]. $PM_{2.5}$ from different sources varies in toxicity due to difference in particle size distributions and chemical composition[28]. Exposure to $PM_{2.5}$ sourced from wildfires has been shown to increase all-cause mortality[29,30], and there is some evidence it is more toxic than $PM_{2.5}$ from other sources[31,32].

Figure 1 uses a geographically-weighted regression surface $PM_{2.5}$ reanalysis dataset[33] (GWR $PM_{2.5}$) to demonstrate the increasing influence of wildfires on summer $PM_{2.5}$ concentrations in the northern hemisphere high-latitudes between 1998 and 2020. Seasonal mean $PM_{2.5}$ peaks during the boreal summer across much of Siberia and Canada (Fig. 1a), suggesting that in these areas wildfires make a dominant contribution to annual $PM_{2.5}$.

[1]Institute for Climate and Atmospheric Science, the University of Leeds, Leeds, UK. [2]National Center for Atmospheric Research, Boulder, CO, USA. [3]Present address: tomorrow.io, Sheffield, UK. ✉e-mail: B.J.Silver@leeds.ac.uk
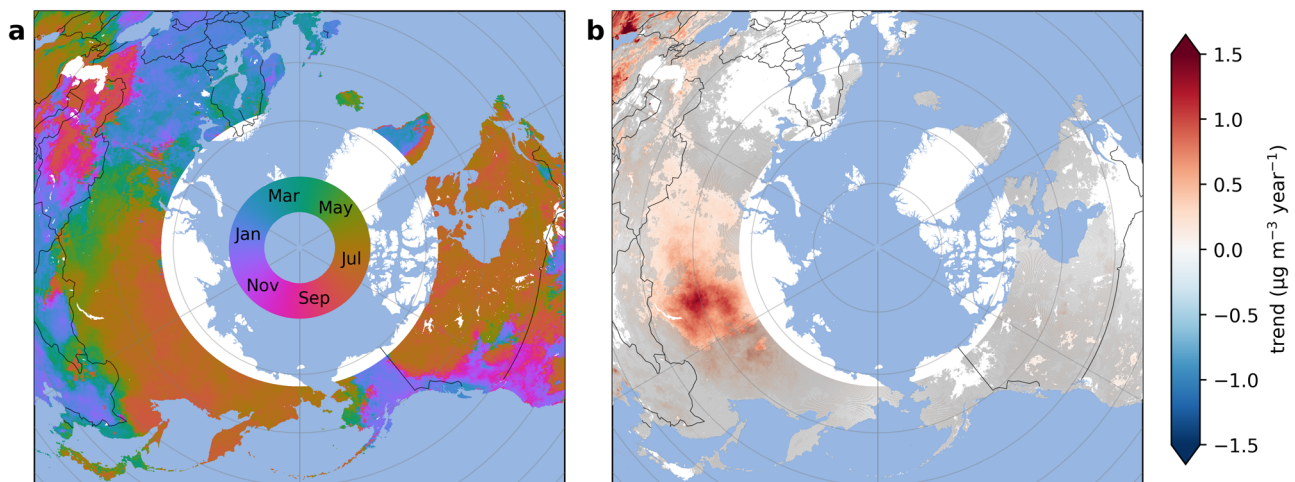
Fig. 1 | Temporal patterns of PM$_{2.5}$ using data from the Geographically Weighted Regression PM$_{2.5}$ dataset[33]. a Average timing of the annual maximum in PM$_{2.5}$ during 1998 to 2020 (**b**) Summer (JJA) PM$_{2.5}$ trend during 1998 to 2020.

Trends are calculated using the Theil-Sen trend estimator[69], and insignificant trends (Mann–Kendall test, $p > 0.05$) are greyed out.

Figure 1b shows there was a positive trend of around 1.5 µg m^{-3} year^{-1} in summer (JJA) PM$_{2.5}$ concentrations in parts of Siberia over the past two decades. This represents a substantial worsening of summer air quality, with parts of the Irkutsk Oblast and Sakha Republic regions of Russia moving from average summer PM$_{2.5}$ concentrations of ~10 µg m^{-3} in 1998 to ~40 µg m^{-3} in 2020.

We aim to quantify the health impacts of wildfire-sourced PM$_{2.5}$ emitted from Arctic Council states, the eight countries that have territories within the Arctic Circle (Canada, Denmark, Finland, Iceland, Norway, Russia, Sweden and the United States), on local and distant populations. The Arctic Council is an intergovernmental forum that promotes cooperation among its members on issues such as community health and sustainable development[34]. Using the Community Earth System Model (CESM) with the Quick Fire Emissions Dataset (QFED)[35], we estimate the contribution of wildfires in the Arctic Council states to high-latitude surface PM$_{2.5}$, and quantify the public health impacts due to long-term ambient PM$_{2.5}$ exposure.

Results
Fire emissions spatial patterns and temporal trends
Spatial and temporal patterns of wildfires and other fires (e.g., agricultural crop burning) in the Arctic Council states for the period 2001–2020 are shown in Fig. 2, based on QFED emissions data and satellite-based land cover classification (see Methods). In the Arctic Council nations, wildfires account for 89% of total carbon released by fires during 2001–2020, which varies annually from 82% to 94%. Most agricultural fires occur south of 55°N, while wildfire emissions extend to 68°N. The majority of agricultural fires occur at the southern perimeter of Arctic Council states, primarily around the Canada-contiguous US border and the Russia-Kazakhstan border. Agricultural fires also appear widespread in southwestern regions of Russia (North Caucasus, Southern and Central Federal districts), which may be attributable to prescribed crop residue burning[36].

Despite the wildfire emissions across the Arctic Council remaining relatively stable during 2001–2020 (Fig. 2), some regions in Russia, i.e., the Sakha Republic, Irkutsk Oblast and Krasnoyarsk Oblast, have a positive trend in annual total wildfire carbon emissions of >4% year^{-1}, though only Krasnoyarsk Oblast has a statistically significant trend (Supplementary Fig. 1).

Wildfire-sourced PM$_{2.5}$
As expected, most of the areas of elevated Arctic wildfire-sourced PM$_{2.5}$ lie within the borders of the Arctic Council states (Fig. 3). On average, wildfire PM$_{2.5}$ accounts for 21% of annual mean PM$_{2.5}$ from all sources within Arctic Council states. In Russia and Canada, wildfires contribute 22.8 and 27.1% of

annual PM$_{2.5}$ on average respectively, while in Scandinavian countries wildfires contribute only ~2%. The areas with the largest wildfire-attributed PM$_{2.5}$ occur in Russia, especially around the Chinese and Mongolian borders, where wildfires add more than 8–10 µg m^{-3} (40–50%) to annual mean PM$_{2.5}$ (Fig. 3). In more remote parts of Siberia and Canada, wildfire-attributed PM$_{2.5}$ accounts for over 70% of annual mean PM$_{2.5}$. China and Mongolia also contain regions where mean PM$_{2.5}$ concentrations are elevated by Arctic wildfires, suggesting that they regularly suffer from episodes of enhanced pollution due to transboundary transport of Arctic wildfire plumes.

In most countries, the proportion of population-weighted mean PM$_{2.5}$ attributed to wildfires is lower, as wildfires tend to occur in less densely populated areas, while the majority of PM$_{2.5}$ exposure occurs in urban areas. Canada and Russia have the highest proportion of their population-weighted mean PM$_{2.5}$ attributed to Arctic wildfires, at 8.7 and 8.2% respectively. Mongolia has the highest population-weighted mean PM$_{2.5}$ attributed to wildfires outside the Arctic Council (Table 1), as its capital city is close to the area of regular Siberian wildfires.

As shown in Fig. 1b, summer (JJA) PM$_{2.5}$ concentrations have been increasing over the period 1998–2020 across much of Siberia, while slightly decreasing in other parts of the Arctic. During this 22-year period, some areas of Siberia show a summer PM$_{2.5}$ trend of >1 µg year^{-1}. Our simulations show that the proportion of wildfire-sourced PM$_{2.5}$ has not changed on average across the Arctic Council states, but has increased by >3% year^{-1} in parts of Siberia (Supplementary Fig. 2). The area in Fig. 1b that shows the most rapid increase in wildfire PM$_{2.5}$ is to the north of Lake Baikal, where a significant increase in fire burned area has been detected during the past two decades[37].

Arctic Council states show different time-evolution of wildfire-sourced PM$_{2.5}$ in populated regions. Figure 4 shows the change in the area-weighted mean and population-weighted mean concentrations of wildfire-sourced PM$_{2.5}$ across each of the Arctic Council states. Where the population-weighted mean PM$_{2.5}$ is larger than the area-weighted mean (e.g., for Norway and Greenland), this indicates the wildfire smoke has a disproportionately elevated impact on populated areas. When the opposite is true (e.g., for Sweden, Russia and Canada), wildfire smoke increases PM$_{2.5}$ concentrations more in less densely populated regions. In Russia, the population-weighted mean PM$_{2.5}$ decreases, while the area-weighted mean PM$_{2.5}$ increases over time. This indicates that despite wildfire PM$_{2.5}$ concentrations increasing on average during 2001–2020, the impact on populated areas in Russia has decreased.

Our analysis indicates a shift in the latitude of wildfire emissions and PM$_{2.5}$ over time in some regions of the high latitudes. Figure 5 shows that areas of wildfire-sourced PM$_{2.5}$ have shifted northwards in much of eastern Russia. As this area has a high proportion of wildfire-sourced PM$_{2.5}$ (Fig. 3a),
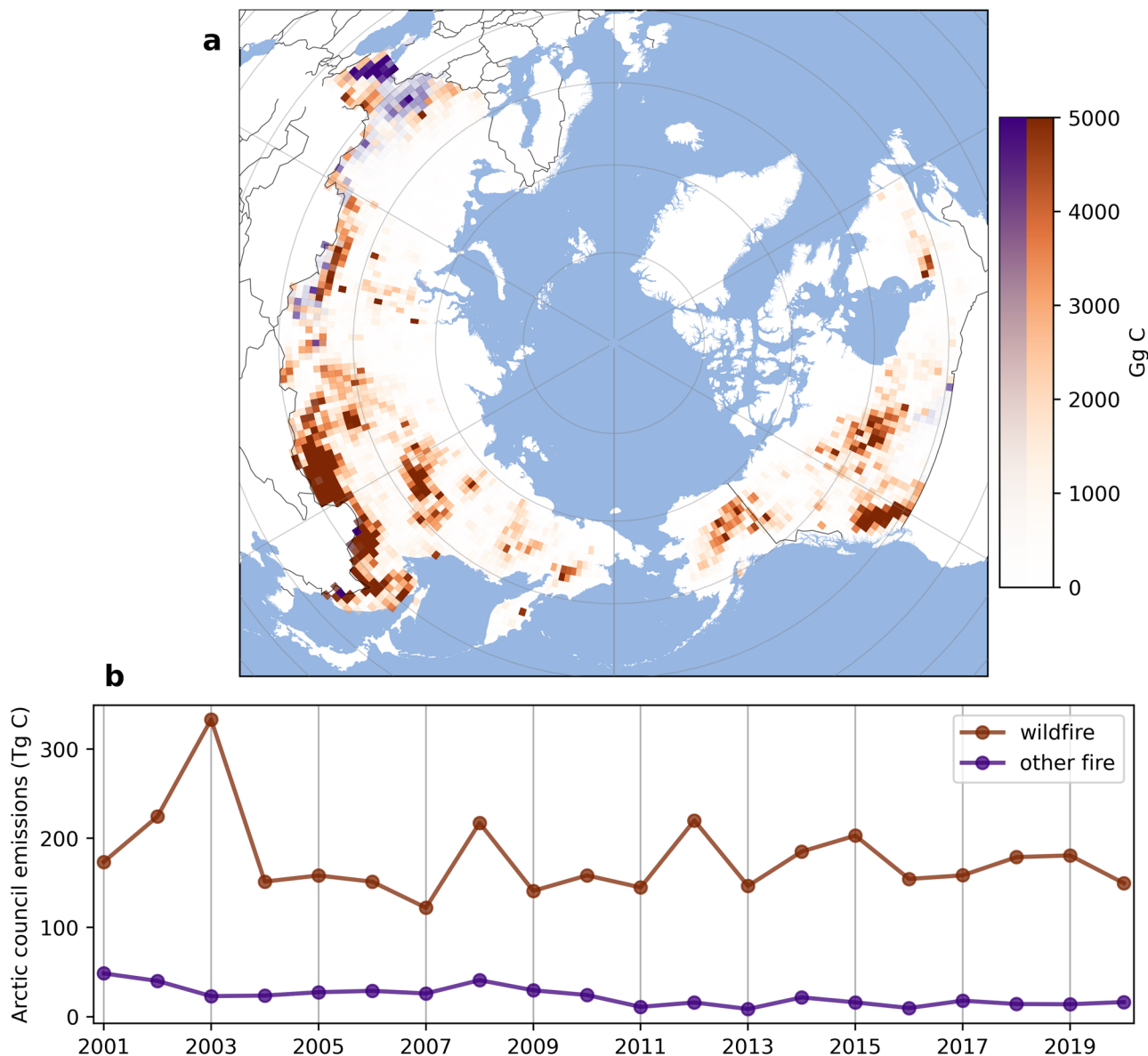
Fig. 2 | Arctic Council wildfire emissions scenarios using data from the Quick Fire Emissions Dataset (QFED, version 2.5)[35]. a Total fire emissions during 2001–2020 from the QFED. Purple shades represent emissions from land classed as agricultural in MODIS, while orange shades represent emissions from non-agricultural land, assumed to be wildfires. **b** Time series showing the total fire emissions (Tg C) per year.

this indicates a shift in the wildfire regime, with wildfires occurring at higher latitudes during the 2011–2020 period compared to 2001–2010, which has been noted in ref. 38.

Wildfire-attributed mortality

Our modelling attributes 21,100 (95% confidence interval (CI): 15,800–27,700) excess deaths to Arctic Council wildfire-sourced PM$_{2.5}$ on average each year, with over a third of the health impact (8100 (95% CI: 5900−10,800) mortalities) occurring in nations outside the Arctic Council (Table 2; Fig. 6). The country that experiences the single largest mortality burden is Russia, with 9900 (7300−13,100) mortalities on average per year (Table 2). In per capita terms, Russia's health impact is also the largest, with around 69 (51−92) annual excess deaths per million people attributed to wildfire PM$_{2.5}$ on average. Among the Arctic Council states, Canada also has a high per capita impact, with 38 (31−46) Arctic wildfire-attributed mortalities per million. Other countries with a high per capita health impact are those bordering or close to Russia, including Mongolia (39 (26−57)), Belarus (26 (18−38)) and Georgia (19 (14−25) mortalities per million).

Although only 0.2% of China's population-weighted mean PM$_{2.5}$ is attributed to Arctic wildfires, it has the second largest mortality burden of 4800 (3500−6400) mortalities attributed to Arctic wildfires on average per year. This is due to its proximity to Siberia; wildfire smoke plumes are advected over north-eastern China, which is a relatively densely populated region, resulting in a larger exposed population and a larger associated mortality burden.

The number of mortalities attributed to Arctic wildfires declines during the period of our study (Fig. 6), with 22,900 (17,300−30,000) excess deaths on average during 2001–2010, and 19,200 (14,200-25,400) during 2011–2020 (Table 2). This is despite the positive trend in summer PM$_{2.5}$ concentrations in some parts of the Arctic shown in Fig. 1. The majority of the decreased health burden occurs in non-Arctic Council states, where Arctic wildfire-sourced PM$_{2.5}$ concentrations have declined, whereas within Arctic Council states annual wildfire-sourced PM$_{2.5}$ concentrations and wildfire-attributed mortalities remain stable over time. Years with larger health impacts outside the Arctic Council are caused by wildfires occurring in areas bordering populous regions of non-Arctic Council states.
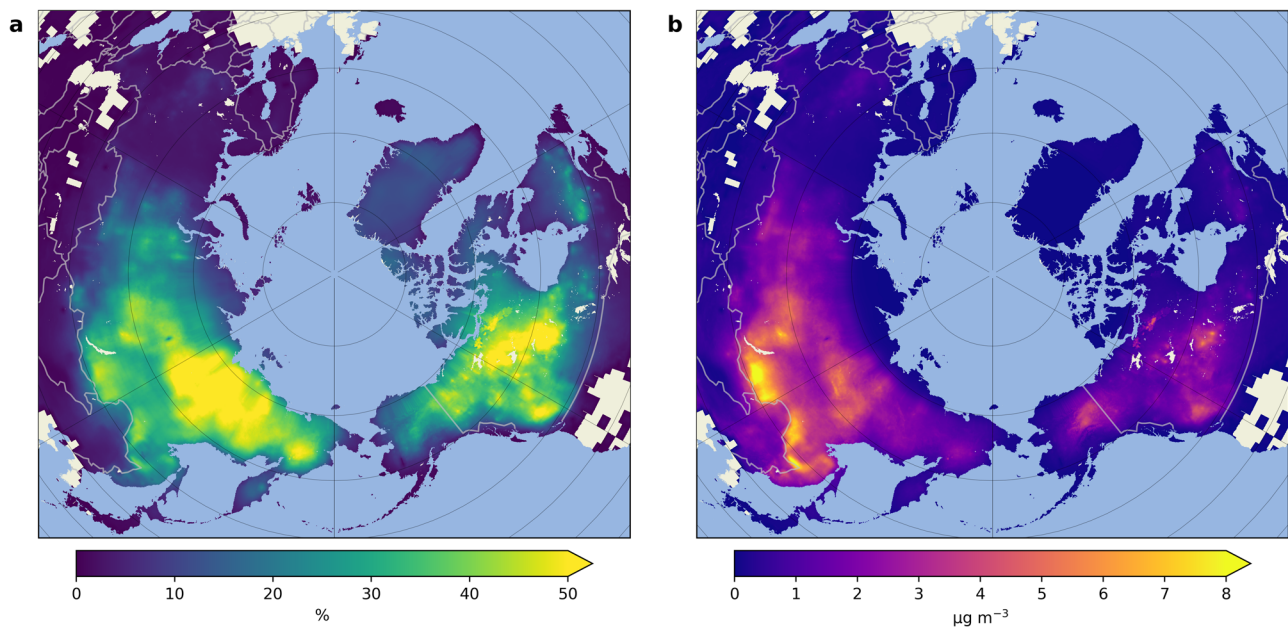
Fig. 3 | Average (during 2001 to 2020) PM$_{2.5}$ increase attributed to wildfires in Arctic Council states. a showing the percentage of PM$_{2.5}$ attributed to Arctic wildfires and (**b**) showing the absolute concentration of wildfire-sourced PM$_{2.5}$. In both panels data is only shown where there is a significant increase in PM$_{2.5}$ attributed to Arctic Council wildfires.

Table 1 | Mean and standard deviation (2001–2020) of PM$_{2.5}$ concentrations (µg m^{-3}) averaged by country

Country	Mean PM$_{2.5}$			Population-weighted mean PM$_{2.5}$		
	Total	Attributed to Arctic wildfires		Total	Attributed to Arctic wildfires	
	µg m^{-3}	µg m^{-3}	% of total	µg m^{-3}	µg m^{-3}	% of total
Russia	7.8 ± 0.9	1.8 ± 0.7	22.8 ± 7.0	14.7 ± 1.2	1.2 ± 0.4	8.2 ± 1.8
USA	7.3 ± 1.1	0.2 ± 0.1	3.3 ± 1.6	9.2 ± 1.7	0.1 ± 0.0	1.1 ± 0.4
Canada	4.1 ± 0.5	1.1 ± 0.4	27.1 ± 7.4	6.8 ± 0.8	0.6 ± 0.1	8.7 ± 2.2
Greenland	1.5 ± 0.1	0.1 ± 0.0	3.8 ± 1.2	1.1 ± 0.1	0.0 ± 0.0	3.5 ± 1.1
Iceland	4.8 ± 0.3	0.0 ± 0.0	0.9 ± 0.6	4.8 ± 0.3	0.0 ± 0.0	0.6 ± 0.6
Norway	5.1 ± 0.5	0.1 ± 0.0	2.0 ± 0.7	6.5 ± 0.8	0.1 ± 0.1	1.8 ± 0.7
Sweden	5.5 ± 0.6	0.1 ± 0.0	2.1 ± 0.7	6.7 ± 0.9	0.1 ± 0.0	1.1 ± 0.4
Finland	5.3 ± 0.7	0.1 ± 0.1	2.5 ± 1.2	6.4 ± 1.0	0.1 ± 0.1	1.5 ± 0.8
Mongolia	19.1 ± 1.5	1.1 ± 0.8	5.7 ± 3.6	37.5 ± 4.0	2.0 ± 1.2	5.3 ± 3.2
Belarus	16.2 ± 1.9	0.5 ± 0.3	2.8 ± 1.6	16.4 ± 1.9	0.5 ± 0.3	2.8 ± 1.6
Georgia	20.8 ± 1.3	0.5 ± 0.2	2.5 ± 1.0	20.5 ± 1.2	0.4 ± 0.2	1.8 ± 0.8
Estonia	9.2 ± 1.4	0.2 ± 0.1	2.2 ± 1.1	7.8 ± 1.3	0.2 ± 0.1	2.0 ± 1.1
Latvia	14.9 ± 1.9	0.3 ± 0.2	2.0 ± 1.0	14.3 ± 1.9	0.2 ± 0.1	1.5 ± 0.7
Japan	11.4 ± 1.1	0.2 ± 0.1	2.0 ± 1.0	12.1 ± 1.0	0.1 ± 0.1	0.8 ± 0.4
Lithuania	15.6 ± 1.9	0.3 ± 0.2	1.8 ± 1.0	15.0 ± 1.9	0.3 ± 0.2	1.9 ± 1.1
Moldova	18.1 ± 1.8	0.3 ± 0.2	1.8 ± 1.2	18.3 ± 1.8	0.4 ± 0.3	2.0 ± 1.3
China	32.2 ± 3.3	0.5 ± 0.3	1.5 ± 0.8	48.7 ± 6.6	0.2 ± 0.1	0.4 ± 0.2

PM$_{2.5}$ concentrations are taken from the scenario with Arctic Council wildfires included, while the 'wildfire-attributed' PM$_{2.5}$ is from the difference between the two scenarios with and without Arctic Council wildfires. Arctic Council states are denoted using bold text, while the other countries shown are the eight countries with the highest proportion of Arctic Council wildfire-sourced PM$_{2.5}$. In addition, China is included due to its high Arctic wildfire-attributed excess deaths.

Discussion

Wildfires account for the majority of annual mean PM$_{2.5}$ across much of the Canadian and Siberian Arctic (Fig. 3a). Due to the sparsely populated nature of these areas, the health impact is relatively low, accounting for <2% of PM$_{2.5}$ attributed excess deaths in all countries except Canada (9%), Russia (6%) and Mongolia (3%). The largest health impacts in absolute terms occur when plumes of wildfire pollution are advected over densely populated areas. However, the populations who experience the largest impacts on a per capita basis from Arctic wildfires live in the remote areas immediately around fires (Supplementary Fig. 3). In some countries, especially Russia, our modelling indicates that the health impact is exacerbated further due to the high underlying baseline rates of mortality.

Our results demonstrate that PM$_{2.5}$ pollution sourced from wildfires inside the Arctic Council states have a substantial transboundary health
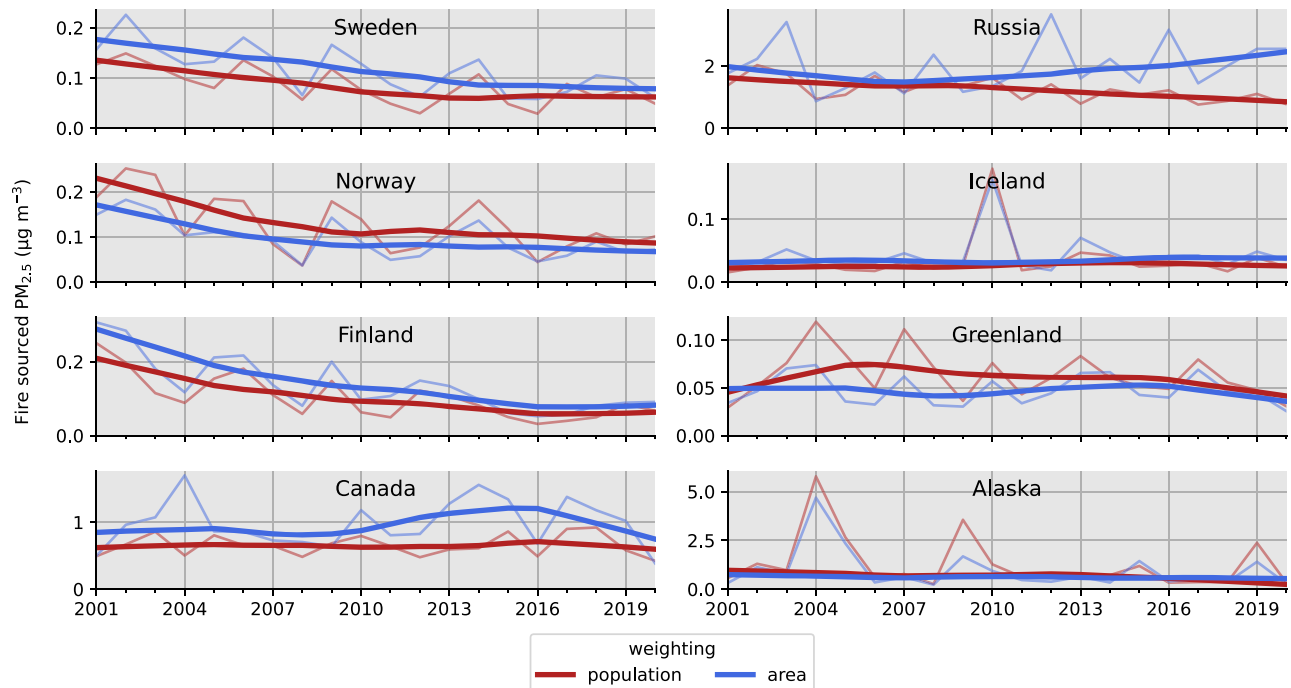
Fig. 4 | Wildfire-sourced PM$_{2.5}$ averaged across each of the Arctic Council states. The PM$_{2.5}$ average weighted by area (blue) and population (red) is shown. The thin lines show the annual means and the thick lines are a smoothed fit.
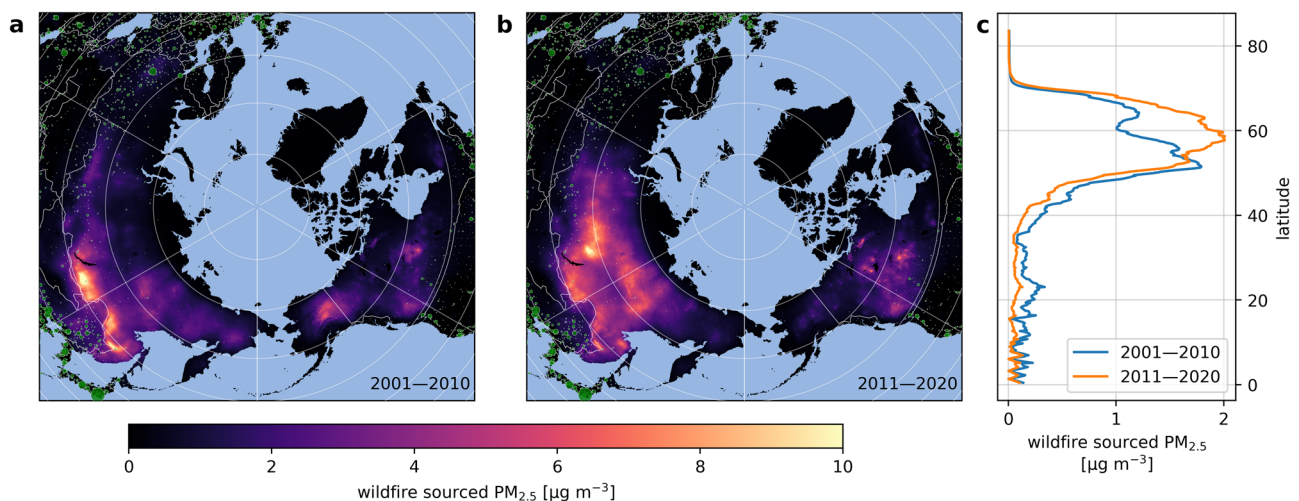
Fig. 5 | Comparison of 2001–2010 and 2011–2020 Arctic wildfire-attributed PM$_{2.5}$. a, **b** show the mean Arctic wildfire-attributed PM$_{2.5}$ during 2001–2010 and 2011–2020, respectively. Green circles are added to show populated places data from Natural Earth (https://www.naturalearthdata.com/downloads/10m-cultural-vectors/10m-populated-places/ (last accessed 13/05/2023)), with circle size determined by relative population count. In (**c**), the wildfire-sourced PM$_{2.5}$ averaged by latitude for each time period are shown.

impact on remote populations, with over a third of Arctic wildfire PM$_{2.5}$-attributed excess deaths occuring in non-Arctic Council states. However, the transboundary impacts appear to have decreased during the last two decades, as Siberian wildfires shift to higher latitudes, away from the Mongolian and Chinese borders with Russia.

Burned area in boreal forests is positively correlated with fire weather index[39]. Fire weather frequency and severity has increased in boreal regions during recent decades[40]. It is not clear to what extent climate change has driven this apparent trend, and therefore whether it could be expected to persist in the future, especially as the response of wildfires and underlying vegetation to climate are highly uncertain[41,42]. It remains to be seen whether the northwards shift in burning will continue over the next years and decades. More work is needed to establish which drivers have led to the strong

positive trend in wildfire-sourced air pollution in some parts of Siberia during the past two decades, and to establish how likely the anomalously large Siberian fires of 2019–20 are to be repeated in the context of a shifting climate.

Our health calculations use the GEMM[23], based on from data 41 epidemiological studies to establish exposure-response curves between annual mean PM$_{2.5}$ concentrations and mortality. These exposure-response curves likely best represent the regions from which most of epidemiological data is collected, i.e., urban regions outside the Arctic. Arctic populations likely have different lifestyle factors (e.g., time spent outdoors, activity rates, public transport use) that may result in a different relationship between ambient air pollutant concentrations and personal exposure. Our population age structure and baseline mortality data are at the national level, so any regional
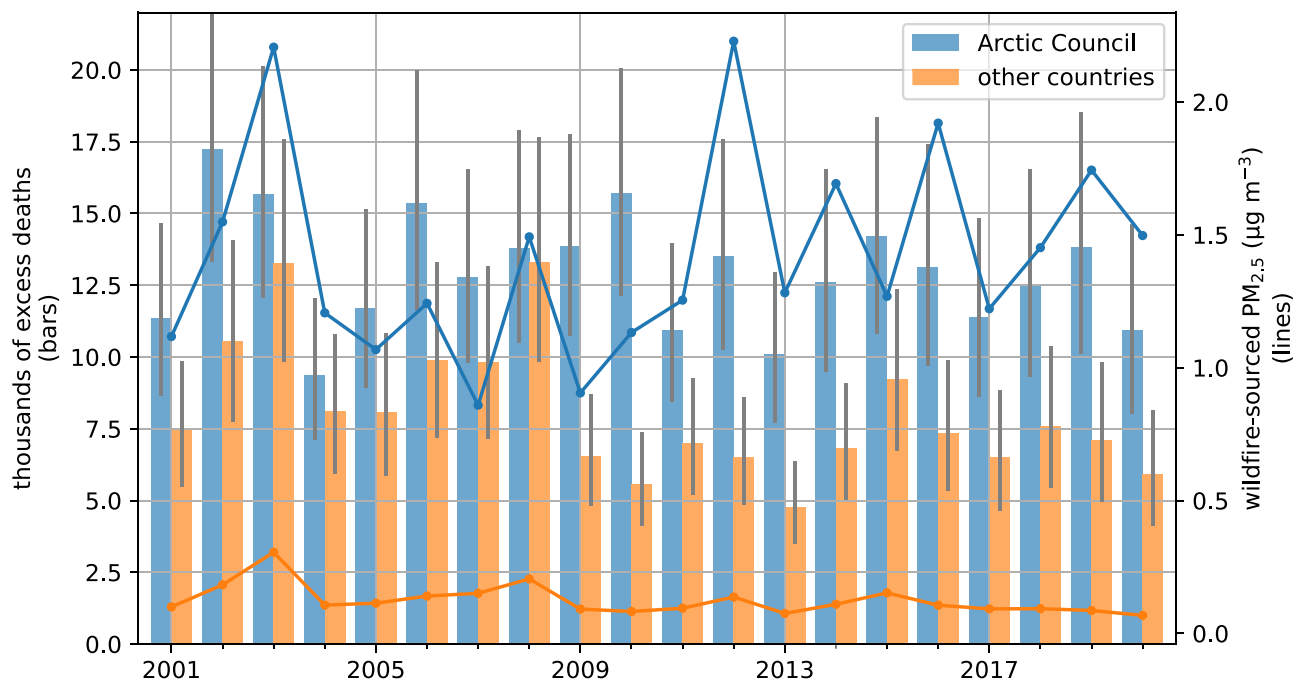
Fig. 6 | Time series of the additional mortalities attributed to Arctic Council wildfires and Arctic wildfire-sourced annual mean PM$_{2.5}$ concentrations. The time series are divided into Arctic Council states (blue) and the rest of the northern hemisphere (orange). The excess deaths are shown as coloured bars with grey error bars showing the upper and lower confidence intervals estimated from the health impact model. The Arctic wildfire-sourced annual mean PM$_{2.5}$ concentrations are shown as lines.

variation in population demographics within countries is not included in this analysis. Sub-national level baseline health data and Arctic wildfire specific PM$_{2.5}$ exposure-response health functions could improve our estimates in future work. Despite these potential limitations, our study provides the first estimate of wildfire health impacts across the Arctic Council states, to the best of our knowledge, based on available information and modelling analyses.

Our simulated PM$_{2.5}$ concentrations have a negative bias when compared to the few available observations within the Arctic (see Section "Correction of simulated PM$_{2.5}$ to observations"), which introduces uncertainty into our estimation of the fire fraction of PM$_{2.5}$, which could further propagate into our health impact estimation. Lack of Arctic PM$_{2.5}$ observations, particularly those of speciated PM$_{2.5}$ makes it difficult to quantify uncertainty in our fire fraction estimate that would propagate into our mortality estimates. However, it is well-established that models tend to underestimate aerosol concentrations in areas of high biomass burning[43–45], it is likely that our mortality estimates are conservative, despite them being larger than those estimated for high-latitude nations in a previous global study, ref. [46]. McDuffie et al. [46] provide by-country totals of their mortality attributed to non-cropland fire emissions in 2017 and 2019, estimated using the GEMM model. We exclude the United States from the comparison, as in our study we do not remove wildfire emissions from the contiguous-United States. For the remaining Arctic Council nations, in 2017 and 2019 our mortality estimates are a factor 2–3 times larger, although we note both chemical transport modelling and fire emissions differ between the two studies. McDuffie et al. [46] use the Global Fire Emissions Dataset version 4[47], which has been shown to underestimate burned area in the high latitudes[48].

The northwards shift in fire emissions and air quality impact in Siberia has caused the overall PM$_{2.5}$-attributable mortality impact of wildfires to decrease, despite the increase in fire emissions in this area[4], mainly due to the reduced impact on relatively densely populated regions such as northeast China and Mongolia. Although this work focuses on the human health impact, shifting Arctic fire regimes will also affect ecosystems that are already vulnerable due to climate change[49,50], and could accelerate the release of carbon stored in tundra ecosystems.

Methods
Model setup
To estimate the impact of Arctic Council wildfires on human mortality, we simulate global PM$_{2.5}$ under two scenarios:

- 'FIRE ON,' a control simulation using the Quick Fire Emissions Dataset (QFED, version 2.5)[35] fire emission dataset, which includes daily fire emissions from all fires (wildfire and agricultural) and all regions.

- 'ARCTIC WILDFIRE OFF,' a counterfactual scenario without wildfire emissions within Arctic Council states, but including other types of fires in the Arctic, and all types of fire outside the Arctic. In this scenario wildfires resulting from both human and natural ignitions are removed.

The eight Arctic Council member states are; Canada, Denmark, Iceland, Norway, Sweden, Finland, Russia and the United States. As we are focussed on the impact of wildfires in high latitude regions, we do not include the contiguous United States or Denmark (but do include Greenland) as Arctic Council areas.

The simulations are performed with the Community Earth System Model (CESM) version 2.2[51] in a configuration which includes the Community Atmosphere Model with chemistry (CAM-Chem) to simulate tropospheric and stratospheric chemistry, and simplified representations of other components of the Earth (e.g., oceans, sea-ice etc.). The version of CAM-chem in CESM v2.2 is CAM6-chem, which uses a recent version of the Model for Ozone and Related chemical Tracers (MOZART) chemical mechanism, MOZART-TS1[52], to represent gaseous species, and a Volatility Basis Set scheme to represent ageing of organic aerosol. The aerosol size distributions are represented using the four-mode version of the Modal Aerosol Model (MAM4)[53], which added an additional mode to improve representation of carbonaceous aerosols, black carbon (BC) and primary organic matter (POM). We run CESM at the standard grid resolution of 0.9° by 1.25° (latitude by longitude), with the meteorology nudged using MERRA2 reanalysis data.

Table 2 | Annual PM$_{2.5}$-attributed excess deaths averaged by country averaged over the 2001–2020 period

country	Mean annual PM$_{2.5}$-attributed deaths	Mean annual Arctic Wildfire-sourced PM$_{2.5}$-attributed deaths	Mean annual Arctic wildfire-sourced PM$_{2.5}$-attributed deaths per thousand population
Russia	174,200 (127,991–233,597)	9878 (7315–13147)	69 (51–92)
USA	193,705 (157,813–234,251)	1699 (1389–2048)	5 (4–7)
Canada	13,889 (11,379–16,701)	1280 (1051–1535)	38 (31–46)
Greenland	0 (0–0)	0 (0–0)	0 (0–0)
Iceland	75 (62–91)	1 (0–1)	2 (1–2)
Norway	2103 (1824–2415)	35 (30–40)	7 (6–8)
Sweden	5013 (4362–5718)	57 (50–65)	6 (5–7)
Finland	2678 (2310–3079)	42 (36–48)	8 (7–9)
Mongolia	3279 (2170–4897)	106 (71–156)	39 (26–57)
Belarus	13,719 (9227–20,210)	250 (169–365)	26 (18–38)
Georgia	6929 (5023–9333)	79 (58–105)	19 (14–25)
Estonia	954 (693–1283)	15 (11–20)	11 (8–15)
Latvia	2675 (2019–3539)	28 (21–36)	14 (10–18)
Japan	103,710 (83,811–126,624)	620 (503–753)	5 (4–6)
Lithuania	3914 (2808–5339)	48 (34–65)	15 (11–21)
Moldova	4766 (3451–6443)	60 (44–80)	16 (11–21)
China	1,835,575 (1,330,014–2,470,032)	4824 (3534–6425)	4 (3–5)

The central estimate from the Global Exposure Mortality Model (GEMM) is shown, followed by the lower and upper confidence intervals (in parentheses). The PM$_{2.5}$ attributed deaths is from the scenario that includes Arctic wildfires (GWR PM$_{2.5}$), while the Arctic wildfire-sourced PM$_{2.5}$-attributed deaths is calculated by subtracting the excess deaths estimated from the 'BIAS CORRECTED WILDFIRE OFF' scenario from the GWR PM$_{2.5}$ scenario. Arctic Council states are denoted using bold text, while the other countries shown are the eight countries with the highest proportion of Arctic Council wildfire-sourced PM$_{2.5}$. In addition, China is included due to its high Arctic wildfire-attributed excess deaths.

Due to coupled chemical and meteorological processes in CESM, changes in the fire emissions between the two scenarios result in small perturbations of meteorological parameters (e.g., temperature, wind speeds), which will in turn affect secondary PM$_{2.5}$ concentrations, which can propagate to regions distant from the Arctic. These fluctuations could be misinterpreted as being directly caused by wildfire-sourced PM$_{2.5}$ when comparing the two scenarios. To focus on the direct impacts of wildfire, we calculate wildfire-attributable PM$_{2.5}$ as the difference in the POM and BC fractions between the two scenarios, which are not affected by secondary aerosol formation or meteorological feedbacks. Since these species represent on average >99.9% of primary aerosol mass emitted by Arctic Council wildfires, this method covers the large majority of the expected driver of PM$_{2.5}$-attributable health impacts.

We also exclude areas where the increase in the POM + BC PM$_{2.5}$ in the FIRE ON scenario is statistically insignificant when compared with the ARCTIC WILDFIRE OFF scenario. We do this by performing a one-sided paired samples t test at each CESM grid cell between the monthly mean concentrations in the two scenarios during the 2001–2020 period, with a significance threshold of $p = 0.01$. If no significant increase is found, we set the 'FIRE FRACTION' term to zero in the bias correction equation (Section "Correction of simulated PM$_{2.5}$ to observations"), resulting in no health impact attributed to wildfires at that location. This ensures that statistically insignificant differences between the two scenarios in more populated regions distant from the Arctic do not unduly contribute to the calculated health impact. The result of the t test are shown in Supplementary Fig. 4.

Developing a 'wildfire off' emissions scenario

Both CESM model simulations include fire emissions from the QFED dataset[35]. In QFED, emissions of gaseous and particulate species released by biomass burning are based on satellite-detected fire radiative power (FRP) observations, along with biome-specific emissions factors that are calibrated by comparing modelled and observed aerosol optical depth (AOD). We chose QFED over other biomass burning emission inventories (BBEIs) as its use of AOD observations can reduce emission underestimation[35,45], and it has been shown to have the lowest negative bias against AOD among six commonly used BBEIs[44], so it is less likely to underestimate PM$_{2.5}$ concentrations, which are the primary focus of this analysis.

However, QFED emission estimates do not discriminate between agricultural and wildfires. Therefore, to construct a biomass burning emissions scenario without wildfires, we assume that emissions from agricultural land are not wildfires, and emissions from other land uses are wildfires.

The resolution of the QFED emissions used has been regridded to CESM resolution (0.9° by 1.25°) while the MODIS land use data is available at 0.01° by 0.01°. Using MODIS data at its native spatial resolution (Supplementary Fig. 5), we calculate the proportion of agricultural land in each QFED grid cell, which is used to fractionally portion the QFED emissions between wildfire and agricultural emissions. The wildfire and cropland attributed emissions are shown in Supplementary Fig. 6. Any error introduced due to the resolution mismatch between QFED and MODIS data will have a relatively small impact on our analysis due to the small fraction of land area with cropland cover in the Arctic Council, most of which is grouped into discrete areas.

Correction of simulated PM$_{2.5}$ to observations

Comparisons with the few available PM$_{2.5}$ observations in the Arctic region show that simulated air pollutant concentrations are persistently underestimated by both regional[54] and global models[55-57]. This is partly due to the difficulty of representing a smoke plume at low resolutions, where the plume will be diluted within a model grid cell. Additionally, biomass burning emissions are often underestimated[43,44,47]. A particular cause of this in the Arctic region could be the peat soils, which frequently experience higher emission smouldering fires, typically not well represented in emission inventories, as they are difficult to detect via satellites[58,59]. Additionally, burned area products derived from satellites can often omit fires due to high detection limits and limited overpass times[60].

The CESM model was compared with a dataset of reference grade PM$_{2.5}$ monitors from the AIRNOW network (north of 55°N), which includes monitors in Alaska, Canada and the US embassy in Almaty, Kazakhstan. CESM has a negative Normalised Mean Bias (NMB) of -0.61 whereas Geographically Weighted Regression (GWR) PM$_{2.5}$[33] has NMB of -0.05 (Supplementary Fig. 7). A similar result was found when comparing the CESM model with a dataset from low-cost '*PurpleAir*' monitors that are located north of 55 N. CESM is negatively biased compared with the *PurpleAir* data (Supplementary Fig. 8), with a NMB of -0.72. The GWR PM$_{2.5}$ product is in closer agreement with the *PurpleAir* monitors with a NMB of 0.1. From these results, we conclude that GWR PM$_{2.5}$ is much better able to represent the magnitude of Arctic PM$_{2.5}$ concentrations than the CESM-simulated PM$_{2.5}$ concentrations.

We use the GWR PM$_{2.5}$ to gain a more accurate estimate of PM$_{2.5}$ concentrations in areas affected by wildfires. This dataset uses satellite AOD observationsalong with model-derived vertical profiles and surface monitoring measurements to estimate monthly mean PM$_{2.5}$ at a resolution of 10 km. However, the FIRE ON simulation underestimates compared with GWR PM$_{2.5}$ in most areas and seasons, not just those affected by wildfire plumes. Therefore, using the ARCTIC WILDFIRE OFF CESM simulation as a counterfactual scenario to be compared with GWR PM$_{2.5}$ would overestimate the fraction of PM$_{2.5}$ that can be attributed to Arctic wildfires.

We use our CESM simulations to estimate the proportion of PM$_{2.5}$ that is attributable to Arctic Council wildfires, which we term the 'FIRE

FRACTION' (Eq. 1). We apply the FIRE FRACTION to the GWR $PM_{2.5}$ data to estimate a counterfactual $PM_{2.5}$ scenario without Arctic wildfires, that we term the 'BIAS CORRECTED WILDFIRE OFF' scenario (Eq. 2).

$$FIRE\ FRACTION = \frac{FIRE\ ON - ARCTIC\ WILDFIRE\ OFF}{FIRE\ ON} \quad (1)$$

$$BIAS\ CORRECTED\ WILDFIRE\ OFF = GWR\ PM_{2.5} \\ \times (1 - FIRE\ FRACTION) \quad (2)$$

The GWR $PM_{2.5}$ reanalysis only extends to 68°N, so at more northerly latitudes the FIRE ON CESM simulation is used. To avoid a hard boundary, we linearly interpolate the GWR $PM_{2.5}$ with the FIRE ON simulation north of 68°N.

Health impact assessment

The health impact of long-term (chronic) exposure to ambient $PM_{2.5}$ concentrations is estimated using the Global Exposure Mortality Model (GEMM)[23] following the method used in previous work[61–63], and other assessments of wildfire smoke health impacts[46,64]. Briefly, using data from 41 epidemiological cohort studies, the GEMM estimates increased relative risk of health impacts from chronic ambient $PM_{2.5}$ exposure above a counterfactual level of 2.4 $\mu g\ m^{-3}$ for adults aged 25 years and older in five-year age groups. We used the relative risk function for non-accidental mortality (including non-communicable disease and lower respiratory infections) and used the parameters that include the China cohort[23]. We use the GEMM because a model that specifically considers the chronic health impact of wildfire smoke is currently not available in the literature. We consider chronic health impacts because across much of the high-latitudes wildfire smoke regularly degrades regional air quality and accounts for a high proportion of annual mean $PM_{2.5}$[65,66].

The Gridded Population of the World (GPW) dataset version 4 was used for population count and distribution[67]. The GPW dataset contains 5-yearly population estimates, which were linearly interpolated to provide the intervening years. The Global Burden of Disease 2019 study data[68] was used for annual population age structure and baseline mortality rates from 2001–2019, with 2020 health impacts calculated using 2019 data.

We use the GEMM to calculate the excess deaths due to chronic $PM_{2.5}$ exposure in both the control scenario (GWR $PM_{2.5}$) and the counterfactual scenario with Arctic Council wildfire pollution removed ("BIAS CORRECTED WILDFIRE OFF", Eq. 2). The difference between the excess deaths under these two scenarios is the mortality burden we attribute to Arctic wildfire smoke. Trend estimations

Trends are calculated using the Theil-Sen trend estimator[69], which is a non-parametric trend estimator that is robust to outliers. Trends were tested for significance using the Mann–Kendall test that detects monotonic increasing or decreasing trends[70].

Reporting summary

Further information on research design is available in the Nature Portfolio Reporting Summary linked to this article.

Data availability

The data used to generate the figures in this study are available to download from Figshare https://doi.org/10.6084/m9.figshare.25325848.v1. The QFED emissions data are available to download from http://ftp.as.harvard.edu/gcgrid/data/ExtData/HEMCO/QFED/v2018-07/. The GWR $PM_{2.5}$ reanalysis data is available to download from https://sites.wustl.edu/acag/datasets/surface-pm2-5/. $PM_{2.5}$ concentration data from the AIRNOW and Purpleair networks are available via their APIs, which are documented at https://docs.airnowapi.org/ and https://api.purpleair.com/, respectively. The GPW data are available from https://sedac.ciesin.columbia.edu/data/collection/gpw-v4. The age structure and baseline mortality data from the Global Burden of Disease 2019 study are available from https://ghdx.healthdata.org/gbd-2019.

Code availability

The CESM is hosted on Github at https://github.com/ESCOMP/CESM and documented at https://www.cesm.ucar.edu/. Model data was analysed using open-source Python packages which are freely available online. The code used to produce the central results of this study is available upon request from the corresponding authors.

References

1. AMAP. Summary For Policy-Makers Arctic Monitoring and Assessment Programme. https://www.amap.no/documents/download/6759/inline (2021).
2. Hantemirov, R. M. et al. Current Siberian heating is unprecedented during the past seven millennia. *Nat. Commun.* **13**, 4968 (2022).
3. Witze, A. The Arctic is burning like never before — and that's bad news for climate change. *Nature* **585**, 336–337 (2020).
4. Descals, A. et al. Unprecedented fire activity above the Arctic Circle linked to rising temperatures. *Science* **378**, 532–537 (2022).
5. Bondur, V. G., Mokhov, I. I., Voronova, O. S. & Sitnov, S. A. Satellite monitoring of siberian wildfires and their effects: features of 2019 anomalies and trends of 20-Year Changes. *Dokl. Earth Sci.* **492**, 370–375 (2020).
6. Climate Watch. Greenhouse Gas (GHG) Emissions. https://www.climatewatchdata.org/ghg-emissions.
7. Turetsky, M. R. et al. Global vulnerability of peatlands to fire and carbon loss. *Nat. Geosci.* **8**, 11–14 (2015).
8. Hugelius, G. et al. Large stocks of peatland carbon and nitrogen are vulnerable to permafrost thaw. *Proc. Natl Acad. Sci.* **117**, 20438–20446 (2020).
9. Andela, N. et al. A human-driven decline in global burned area. *Science* **356**, 1356–1362 (2017).
10. Zheng, B. et al. Increasing forest fire emissions despite the decline in global burned area. *Sci. Adv.* **7**, eabh2646 (2021).
11. Young, A. M., Higuera, P. E., Duffy, P. A. & Hu, F. S. Climatic thresholds shape northern high-latitude fire regimes and imply vulnerability to future climate change. *Ecography* **40**, 606–617 (2017).
12. Stocks, B. J. et al. Climate change and forest fire potential in Russian and Canadian boreal forests. *Clim. Change* **38**, 1–13 (1998).
13. van der Werf, G. R. et al. Global fire emissions and the contribution of deforestation, savanna, forest, agricultural, and peat fires (1997–2009). *Atmos. Chem. Phys.* **10**, 11707–11735 (2010).
14. Lin, S., Liu, Y. & Huang, X. Climate-induced Arctic-boreal peatland fire and carbon loss in the 21st century. *Sci. Total Environ.* **796**, 148924 (2021).
15. Ponomarev, E., Yakimov, N., Ponomareva, T., Yakubailik, O. & Conard, S. G. Current trend of carbon emissions from wildfires in Siberia. *Atmosphere* **12**, 559 (2021).
16. Amiro, B. D., Cantin, A., Flannigan, M. D. & de Groot, W. J. Future emissions from Canadian boreal forest fires. *Can. J. For. Res.* **39**, 383–395 (2009).
17. Ikeda, K. & Tanimoto, H. Exceedances of air quality standard level of PM2.5 in Japan caused by Siberian wildfires. *Environ. Res. Lett.* **10**, 105001 (2015).
18. Mölders, N. & Kramm, G. Climatology of air quality in arctic cities—inventory and assessment. *Open J. Air Pollut.* **7**, 48–93 (2018).
19. Damoah, R. et al. Around the world in 17 days - hemispheric-scale transport of forest fire smoke from Russia in May 2003. *Atmos. Chem. Phys.* **4**, 1311–1321 (2004).
20. Parrington, M. et al. Ozone photochemistry in boreal biomass burning plumes. *Atmos. Chem. Phys.* **13**, 7321–7341 (2013).
21. Wentworth, G. R., Aklilu, Y., Landis, M. S. & Hsu, Y.-M. Impacts of a large boreal wildfire on ground level atmospheric concentrations of PAHs, VOCs and ozone. *Atmos. Environ.* **178**, 19–30 (2018).

22. Lutsch, E. et al. Detection and attribution of wildfire pollution in the Arctic and northern midlatitudes using a network of Fourier-transform infrared spectrometers and GEOS. *Chem. Atmos. Chem. Phys.* **20**, 12813–12851 (2020).

23. Burnett, R. et al. Global estimates of mortality associated with longterm exposure to outdoor fine particulate matter. *Proc. Natl Acad. Sci. USA.* **115**, 9592–9597 (2018).

24. Abbafati, C. et al. Global burden of 87 risk factors in 204 countries and territories, 1990–2019: a systematic analysis for the Global Burden of Disease Study 2019. *Lancet* **396**, 1223–1249 (2020).

25. Lelieveld, J., Evans, J. S., Fnais, M., Giannadaki, D. & Pozzer, A. The contribution of outdoor air pollution sources to premature mortality on a global scale. *Nature* **525**, 367–371 (2015).

26. Thangavel, P., Park, D. & Lee, Y.-C. Recent insights into Particulate Matter (PM2.5)-mediated toxicity in humans: An Overview. *Int. J. Environ. Res. Public. Health* **19**, 7511 (2022).

27. Kim, K. H., Kabir, E. & Kabir, S. A review on the human health impact of airborne particulate matter. *Environ. Int.* **74**, 136–143 (2015).

28. Park, M. et al. Differential toxicities of fine particulate matters from various sources. *Sci. Rep.* **8**, 17007 (2018).

29. Reid, C. E. et al. Critical review of health impacts of wildfire smoke exposure. *Environ. Health Perspect.* **124**, 1334–1343 (2016).

30. Chen, G. et al. Mortality risk attributable to wildfire-related PM2·5 pollution: a global time series study in 749 locations. *Lancet Planet. Health* **5**, e579–e587 (2021).

31. Aguilera, R., Corringham, T., Gershunov, A. & Benmarhnia, T. Wildfire smoke impacts respiratory health more than fine particles from other sources: observational evidence from Southern California. *Nat. Commun.* **12**, 1493 (2021).

32. Stowell, J. D. et al. Associations of wildfire smoke PM2.5 exposure with cardiorespiratory events in Colorado 2011–2014. *Environ. Int.* **133**, 105151 (2019).

33. van Donkelaar, A., Martin, R. V., Li, C. & Burnett, R. T. Regional estimates of chemical composition of fine particulate matter using a combined geoscience-statistical method with information from satellites, models, and monitors. *Environ. Sci. Technol.* **53**, 2595–2611 (2019).

34. The Arctic Council. *Arctic Council* https://arctic-council.org/.

35. Koster, R. D., Darmenov, A. S. & da Silva, A. M. *The Quick Fire Emissions Dataset (QFED): Documentation of Versions 2.1, 2.2 and 2.4.* https://ntrs.nasa.gov/citations/20180005253 (2015).

36. Glushkov, I. et al. Spring fires in Russia: results from participatory burned area mapping with Sentinel-2 imagery. *Environ. Res. Lett.* **16**, 125005 (2021).

37. Tomshin, O. & Solovyev, V. Spatio-temporal patterns of wildfires in Siberia during 2001–2020. *Geocarto Int.* **37**, 7339–7357 (2022).

38. Kharuk, V. I., Dvinskaya, M. L., Im, S. T., Golyukov, A. S. & Smith, K. T. Wildfires in the Siberian Arctic. *Fire* **5**, 106 (2022).

39. Bedia, J. et al. Global patterns in the sensitivity of burned area to fire-weather: implications for climate change. *Agric. For. Meteorol.* **214–215**, 369–379 (2015).

40. Jones, M. W. et al. Global and regional trends and drivers of fire under climate change. *Rev. Geophys.* **60**, e2020RG000726 (2022).

41. Tchebakova, N. M., Parfenova, E. & Soja, A. J. The effects of climate, permafrost and fire on vegetation change in Siberia in a changing climate. *Environ. Res. Lett.* **4**, 045013 (2009).

42. Soja, A. J. et al. Climate-induced boreal forest change: predictions versus current observations. *Glob. Planet. Change* **56**, 274–296 (2007).

43. Reddington, C. L. et al. Analysis of particulate emissions from tropical biomass burning using a global aerosol model and long-term surface observations. *Atmos. Chem. Phys.* **16**, 11083–11106 (2016).

44. Pan, X. et al. Six global biomass burning emission datasets: intercomparison and application in one global aerosol model. *Atmos. Chem. Phys.* **20**, 969–994 (2020).

45. Zhong, Q. et al. Satellite-based evaluation of AeroCom model bias in biomass burning regions. *Atmos. Chem. Phys.* **22**, 11009–11032 (2022).

46. McDuffie, E. E. et al. Source sector and fuel contributions to ambient PM2.5 and attributable mortality across multiple spatial scales. *Nat. Commun.* **12**, 3594 (2021).

47. van der Werf, G. R. et al. Global fire emissions estimates during 1997–2016. *Earth Syst. Sci. Data* **9**, 697–720 (2017).

48. Blackford, K. R. et al. INFERNO-Peat v1.0.0: A Representation of Northern High Latitude Peat Fires in the JULES-INFERNO Global Fire Model. https://egusphere.copernicus.org/preprints/2023/egusphere-2023-2399/, https://doi.org/10.5194/egusphere-2023-2399 (2023).

49. Kirdyanov, A. V. et al. Ecological and conceptual consequences of Arctic pollution. *Ecol. Lett.* **23**, 1827–1837 (2020).

50. Sanderfoot, O. V. et al. A review of the effects of wildfire smoke on the health and behavior of wildlife. *Environ. Res. Lett.* **16**, 123003 (2022).

51. Danabasoglu, G. et al. The Community Earth System Model Version 2 (CESM2). *J. Adv. Model. Earth Syst.* **12**, e2019MS001916 (2020).

52. Emmons, L. K. et al. The Chemistry Mechanism in the Community Earth System Model Version 2 (CESM2). *J. Adv. Model. Earth Syst.* **12**, e2019MS001882 (2020).

53. Liu, X. et al. Description and evaluation of a new four-mode version of the Modal Aerosol Module (MAM4) within version 5.3 of the community atmosphere model. *Geosci. Model Dev.* **9**, 505–522 (2016).

54. Han, K. M. et al. Data assimilation of AOD and estimation of surface particulate matters over the Arctic. *Appl. Sci.* **11**, 1959 (2021).

55. Huang, K. H. et al. Identification of missing anthropogenic emission sources in russia: implication for modeling Arctic Haze. *Aerosol Air Qual. Res.* **14**, 1799–1811 (2014).

56. Eckhardt, S. et al. Current model capabilities for simulating black carbon and sulfate concentrations in the Arctic atmosphere: a multi-model evaluation using a comprehensive measurement data set. *Atmos. Chem. Phys.* **15**, 9413–9433 (2015).

57. Monks, S. A. et al. Multi-model study of chemical and physical controls on transport of anthropogenic and biomass burning pollution to the Arctic. *Atmos. Chem. Phys.* **15**, 3575–3603 (2015).

58. Schmale, J. et al. Local Arctic air pollution: a neglected but serious problem. *Earths Future* **6**, 1385–1412 (2018).

59. McCarty, J. L. et al. Reviews and syntheses: Arctic fire regimes and emissions in the 21st century. *Biogeosciences* **18**, 5053–5083 (2021).

60. Xu, W., Scholten, R. C., Hessilt, T. D., Liu, Y. & Veraverbeke, S. Overwintering fires rising in eastern Siberia. *Environ. Res. Lett.* **17**, 045005 (2022).

61. Conibear, L., Butt, E. W., Knote, C., Arnold, S. R. & Spracklen, D. V. Residential energy use emissions dominate health impacts from exposure to ambient particulate matter in India. *Nat. Commun.* https://doi.org/10.1038/s41467-018-02986-7 (2018).

62. Silver, B. et al. Pollutant emission reductions deliver decreased PM2.5-caused mortality across China during 2015-2017. *Atmos. Chem. Phys.* **20**, 11683–11695 (2020).

63. O'Dell, K. et al. Estimated mortality and morbidity attributable to smoke plumes in the United States: not Just a Western US Problem. *GeoHealth* **5**, e2021GH000457 (2021).

64. Roberts, G. & Wooster, M. J. Global impact of landscape fire emissions on surface level PM2.5 concentrations, air quality exposure and population mortality. *Atmos. Environ.* **252**, 118210 (2021).

65. Sobhani, N., Kulkarni, S. & Carmichael, G. R. Source sector and region contributions to black carbon and PM$_{2.5}$ in the Arctic. *Atmos. Chem. Phys.* **18**, 18123–18148 (2018).

66. Winiger, P. et al. Source apportionment of circum-Arctic atmospheric black carbon from isotopes and modeling. *Sci. Adv.* **5**, eaau8052 (2019).

67. CIESIN. Gridded Population of the World, Version 4 (GPWv4): Population Count. https://doi.org/10.7927/H4X63JVC (2016).
68. Global Burden of Disease Collaborative Network. Global Burden of Disease Study 2019 (GBD 2019) Population Estimates 1950-2019. *Inst. Health Metr. Eval. IHME*. https://doi.org/10.6069/7EGY-0354 (2020).
69. Sen, P. K. Estimates of the regression coefficient based on Kendall's Tau. *J. Am. Stat. Assoc.* **63**, 1379–1389 (1968).
70. Carslaw, D.C. The openair manual — open-source tools for analysing air pollution data. Manual for version 2.6-6, University of York. Available at: https://davidcarslaw.com/files/openairmanual.pdf (2019).

Author contributions
B.S. and S.R.A. conceptualised and designed the study with C.L.R. and L.K.E. providing input. B.S. conducted model simulations and performed health impact analysis with S.R.A., L.K.E. and L.C. providing advice. B.S. performed the data analysis and produced the figures. B.S., S.R.A. and C.L.R. wrote the manuscript. All authors commented on the text.

Competing interests
The authors declare no competing interests.

Additional information
Supplementary information The online version contains supplementary material available at https://doi.org/10.1038/s43247-024-01361-3.

Correspondence and requests for materials should be addressed to Ben Silver.

Peer review information *Communications Earth & Environment* thanks the anonymous reviewers for their contribution to the peer review of this work. Primary Handling Editors: Mengze Li and Clare Davis. A peer review file is available.

Reprints and permissions information is available at http://www.nature.com/reprints

Publisher's note Springer Nature remains neutral with regard to jurisdictional claims in published maps and institutional affiliations.